Optical Materials 59 (2016) 83–86

Contents lists available at ScienceDirect

Optical Materials

journal homepage: www.elsevier.com/locate/optmat

# Photostimulated luminescence properties of neutron image plates

A.I. Popov [a,b,*], J. Zimmermann [c,d], G.J. McIntyre [e], C. Wilkinson [b]

[a] Institute of Solid State Physics, University of Latvia, Kengaraga Str. 8, Riga LV-1063, Latvia
[b] Institut Laue-Langevin, 71, avenue des Martyrs, 38000 Grenoble, France
[c] Institut für Materialwissenschaft, Technische Universität Darmstadt, Petersenstrasse 23, 64287 Darmstadt, Germany
[d] Fraunhofer-Institut für Silicatforschung ISC, Brentanostr. 2, 63755 Alzenau, Germany
[e] The Bragg Institute, ANSTO, Locked Bag 2001, Kirrawee DC, NSW 2232, Australia

ARTICLE INFO

*Article history:*
Received 31 October 2015
Received in revised form 4 January 2016
Accepted 20 January 2016
Available online 25 January 2016

*Keywords:*
Photostimulated luminescence
BaFBr
Storage phosphor

ABSTRACT

The luminescence properties of two commercial neutron-sensitive image-plates based on $Gd_2O_3$-doped BaFBr:$Eu^{2+}$ storage phosphors are examined. These are white Fuji plates and blue Fuji plates (BAS-ND) with $Gd_2O_3$ content by weight of 34% and 50%, respectively. Both plates show two maxima in the photostimulation spectrum near 500 nm and 600 nm, with the ratio of the peak responses ($I_{600\ nm}/I_{500\ nm}$) 1.39 and 0.53 for the white and blue plates respectively. The optimum wavelengths for photostimulation for the two phosphors are therefore different. The response of the blue plate is only 25% that of the white plate, if each is stimulated at its optimum wavelength.



## 1. Introduction

A great deal of research has been performed during the last two decades on photostimulated luminescence and photostimulable storage phosphors [1–15]. Such materials can find attractive application in many different fields of radiation imaging.

When a storage phosphor (e.g. BaFBr:Eu) is mixed with a neutron converter (e.g. $Gd_2O_3$ or LiF), it becomes sensitive to thermal neutrons [16–20]. Neutron-sensitive image plates (NIP's), made of such storage phosphors, have great potential as two-dimensional integrating thermal-neutron detectors [16–20]. Before 2007, there were two neutron image-plate diffractometers at the Institute Laue-Langevin (ILL): LADI (Laue diffractometer) [18], located on a cold-neutron beam, and VIVALDI (Very Intense Vertical Axis Laue Diffractometer) [21], located on a thermal-neutron beam, both of which have been proven to give quantitative structural information in various biological, chemical and magnetic studies [18,21,22]. In 2007 LADI has been replaced by LADI-III image plate diffractometer [22].

On LADI, four $Gd_2O_3$-doped BaF(Br,I):$Eu^{2+}$ Fuji image plates of dimensions 400 mm × 200 mm are bonded onto the outer surface of the cylindrical detector drum. These plates have a $Gd_2O_3$ content of 34% by weight, a detective quantum efficiency of ~20% and a point-spread function of ~100 μm [23]. Their active surface is white, so we will hereinafter refer to them as White NIP's.

On VIVALDI, commercial NIP's (Fuji BAS-ND), also dimensions 400 mm × 200 mm in area, were installed and used during the first 2.5 years of operation (2001–2004). Their active surface is blue, so we will hereinafter refer to them as Blue NIP's. Some properties of the commercial Blue NIP's have been reported by [24]. In these plates the BaFBr:$Eu^{2+}$ phosphor/$Gd_2O_3$ converter ratio is 50/50 by weight. The thickness of the phosphor layer is 135 μm, and is covered by a 6 μm thick polyethylene-terephthalate (PET) protective layer. The support is a (black) 190 μm thick PET film. A ferrite layer is also attached to the rear of the IP for ease of mounting and manipulation in cameras and readers by using the magnetic properties of ferrite. The structure of the Blue NIP is shown in Fig. 1. The blue-colored[1] IP's were developed for transmission electron microscopy with the aim to improve the spatial resolution, and subsequently applied to synchrotron protein crystallography [25,26]; it has been reported that blue X-ray IP's provide a twice better spatial resolution than that provided by conventional white X-ray IP's, possibly via suppression of laser light scattering within the IP without loss of sensitivity [26]. While the improved resolution can be very advantageous for X-ray crystallography and radiography with either X-rays or neutrons, it is less so for neutron crystallography where the reflection size is dominated by the crystal size, which is rarely less than 0.1 mm.

* Corresponding author at: Institute of Solid State Physics, University of Latvia, Kengaraga Str. 8, Riga LV-1063, Latvia.
*E-mail addresses:* popov@ill.fr, popov@latnet.lv (A.I. Popov).

[1] For interpretation of color in Fig. 1, the reader is referred to the web version of this article.

http://dx.doi.org/10.1016/j.optmat.2016.01.038
0925-3467/

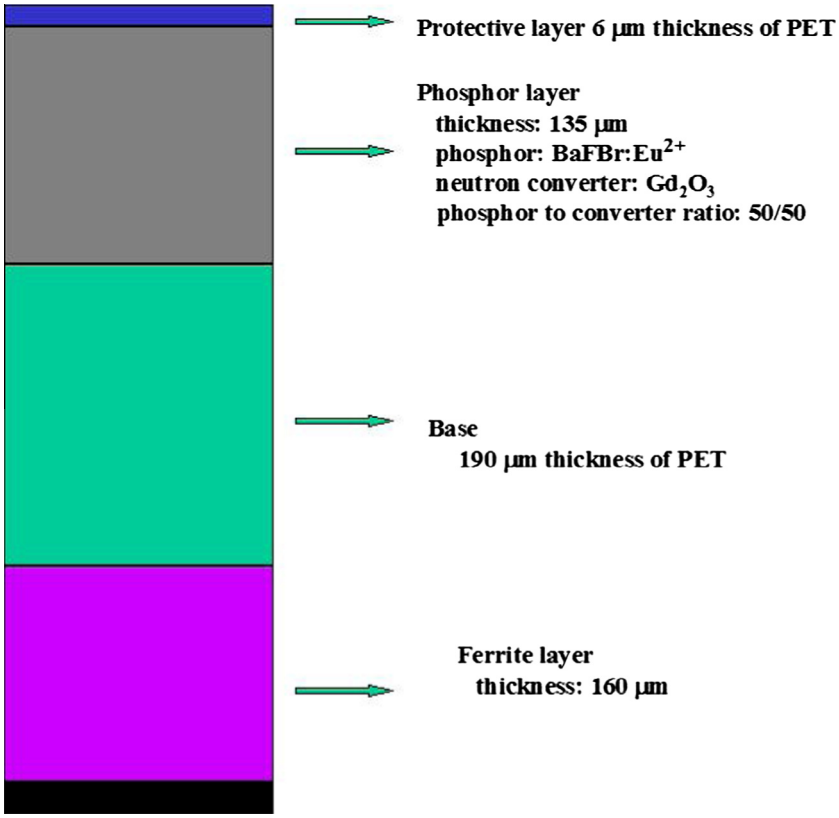


**Fig. 1.** Structure of the Fuji BAS-ND image plate.

The aim of this work was to evaluate the luminescence characteristics of Blue and White NIP's, and thus to find for them the optimal conditions for both stimulation and detection of photostimulated luminescence (abbreviated to PSL stimulation and PSL detection).

## 2. Experimental

X-ray irradiation was performed by a medical X-ray tube with a tungsten anode (Polymobil, Siemens AG) utilizing an acceleration voltage of 90 kV, a 1.4 mm Al filter and a beam current of 16 mA. PSL-stimulation spectra were measured on samples exposed to an X-ray dose of 370 mGy. For PSL excitation of storage centers, light from a 75 W Xenon lamp (Hamamatsu L2174) was dispersed through a monochromator (Jobin-Yvon model DH10UV), chopped and focussed onto the sample. The PSL was collected by means of a photomultiplier (Hamamatsu Model R4220), and the signal was recorded by a lock-in amplifier. The intensity of excitation light was calibrated by means of a Si photodiode. A combination of blue glass filters (Schott) between the sample and the photomultiplier was used to separate the excitation light from the emitted light. X-ray excited luminescence spectra were detected by an optical multichannel analyzer (Spectroscopy Instruments). Photoluminescence excitation and emission spectra have been measured utilizing a Cary Eclipse Spectrometer (Varian).

## 3. Results and discussion

Upon X-ray irradiation electron–hole pairs are generated in a storage phosphor. These then recombine either by emission of spontaneous luminescence, or by generation of a latent image which consists of pairs of electron/hole color centers. As shown in Fig. 2, the spontaneous luminescence emission consists of a single band at 3.10 eV (400 nm) with a half-width of 0.25 eV, which corresponds to the $4f^6 5d^1 \rightarrow 4f^7(^8S_{7/2})$ transition of $Eu^{2+}$ ions, which substitute for Ba ions [1]. Subsequent optical excitation of the color centers leads to the release of trapped electrons and their further recombination with trapped holes giving luminescence. The resulting stimulation spectra give unique information on the electron centers responsible for PSL in a particular storage phosphor. It is generally accepted that the stimulation spectrum is determined by the optical absorption spectrum of the *F*-type centers in BaFX (X = Cl, Br, I) storage phosphors [1,2,4,5,8,10], by both *F*-type centers and/or impurities with trapped electrons in alkali

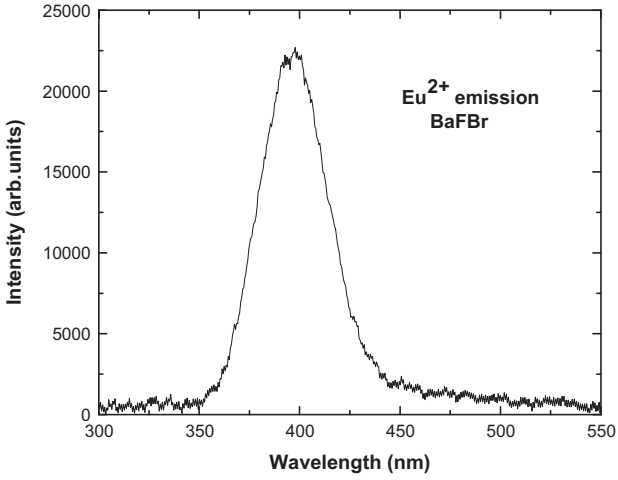


**Fig. 2.** Spontaneous luminescence spectrum of the White NIP under X-ray excitation.

halides [3,7,8,11,27,28], and mostly by impurities with trapped electrons in double-activated sulfides and related materials [6,15,29,30].

Since the stimulation spectra give direct information about defects participating in PSL, we have measured them for both NIP's. The small pieces of the NIPs samples were first irradiated with an X-ray and then the samples were stimulated by monochromatic light in the wavelength regime from 450 to 800 nm. The PSL was detected in the region of $Eu^{2+}$ emission using a photomultiplier (Hamamatsu Model R4220) through a combination of optical filters BG 3/BG 39/UG 1 (Schott). The results are shown in Fig. 3. Two general conclusions can be drawn here. First, the White NIP produces more PSL photons than the Blue NIP over the whole range of the stimulation spectrum (450–800 nm). Secondly, the shapes of their stimulation spectra are quite different. In case of the White NIP the low-energy part of the stimulation spectrum is more pronounced, whereas the stimulation spectrum of the Blue NIP shows the opposite.

For identification of the electron centers responsible for PSL, Gaussian deconvolution of both spectra with energy as the ordinate has been performed. The results are indicated in Fig. 3 and the fitted parameters are listed in Table 1. In both cases the analysis shows that there are two stimulation bands, namely at 2.09 eV (598 nm) and 2.53 eV (490 nm) for the Blue NIP and at 2.08 eV (596 nm) and 2.49 eV (498 nm) for the White NIP.

There is broad agreement that the photostimulation spectrum for BaFBr consists of two broad peaks centered approximately at 500 nm and 600 nm, although the relative amplitudes of these peaks vary considerably in the literature. The heights of the two peaks are reported to be of similar size by Takahashi et al. [1] and by Rüter et al. [4], while Thoms et al. [5], Starick et al. [31] and Iwabuchi et al. [32] report a ratio of approximately 1:2. Our observations for the White NIP are in agreement with the latter observation.

Results where the 500 nm peak is almost absent were reported by Hangleiter et al. [33] and by De Leeuw et al. [2]. Only Su et al. [34] found increased sensitivity at 500 nm. Our observations for the Blue NIP show behavior similar to [34]. The relative heights have been reported to depend on phosphor composition [32,34], its preparation [35] or previous heat treatment [36].

It is generally agreed that the observed stimulation spectrum for PSL is determined by the absorption spectra of the various F-center species created in the phosphor and that the absorption band at 600 nm is due to $F(Br^-)$, where an electron is bound to a $Br^-$ vacancy, while the absorption band at 500 nm is due to F ($F^-$), where an electron is trapped on a $F^-$ vacancy. Thus we can conclude that the concentration of bromine vacancies or the efficiency of F-center creation in the bromine sublattice is higher in the storage phosphor used in the White NIP, whereas in the case of the Blue NIP the reverse is true. Taking into account that under He-Ne laser stimulation mostly $F(Br^-)$-type centers are excited, it is apparent that the phosphor composition used in White NIP's (which were available by special arrangement from Fuji) is to be preferred.

The consequence of different phosphor compositions is seen not only in the stimulation spectra, but also in the photoluminescence spectra. To illustrate this fact photoluminescence spectra of White and Blue NIP's, under ultra-violet (UV) excitation at $\lambda$ = 193 nm, are shown in Fig. 4. In contrast to X-ray excitation, when a single $Eu^{2+}$ band is usually observed (Fig. 1), two emission bands are excited by UV light. The main band corresponds to $Eu^{2+}$ emission, while the shoulder at 2.6–2.7 eV corresponds to BaFBr emission of $O_F^{2-}$ centers [37,38]. Incorporation of $O^{2-}$ ions on fluorine lattice sites, thus requiring anion vacancies for charge compensation, has been considered to be a major relevance for the generation of $F(Br^-)$ [39,40]. The role of oxygen in the PSL process, other than its role

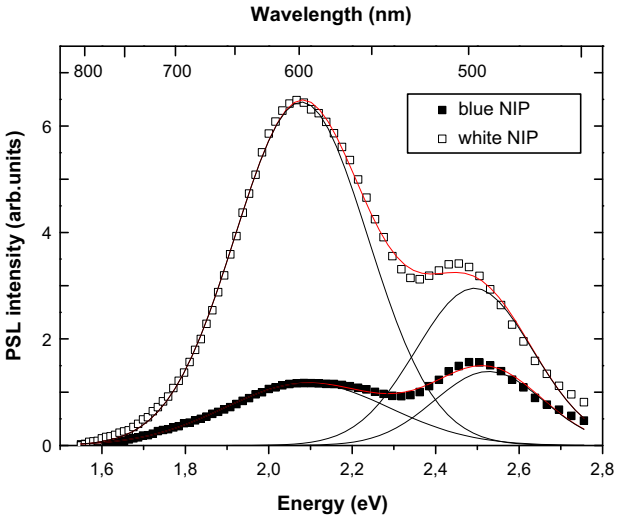


**Fig. 3.** Stimulation spectra of X-ray irradiated Blue and White NIP's and their Gaussian deconvolution. The stimulation spectra were observed by measuring the PSL emission of $Eu^{2+}$ at about 400 nm.

**Table 1**
The fitted parameters of the stimulation spectra of Blue and White NIP's.

| | $E_1$ (eV) | $\Delta E_1$ (eV) | $E_2$ (eV) | $\Delta E_2$ (eV) | $A_1/A_2$ |
|---|---|---|---|---|---|
| Blue NIP | 2.09 | 0.39 | 2.53 | 0.26 | 0.85 |
| White NIP | 2.08 | 0.31 | 2.49 | 0.28 | 2.20 |

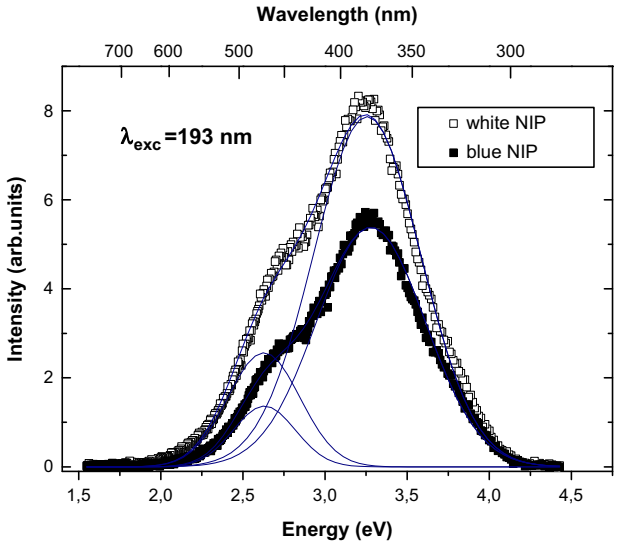


**Fig. 4.** Photoluminescence spectra of White and Blue NIP's under UV-light excitation ($\lambda$ = 193 nm) and their Gaussian deconvolution.

in $F(Br^-)$ formation, is still unclear in detail, although it has been discussed more than once [35,39–41].

From Gaussian deconvolution the relative intensities $I_{Eu}/I_{oxygen}$ are found to be 2.95 and 3.85 for the White and Blue NIP's, respectively. This probably means that the concentration of $Eu^{2+}$ in comparison with the concentration of oxygen centers is higher in the Blue NIP.

From Fig. 3 we can see that the relative PSL intensity of the White NIP is 5.25 times higher than that of the Blue NIP, when the plates are stimulated with a wavelength corresponding to that of a He-Ne laser. The dye contained in the Blue NIP's will also

absorb stimulating photons in the red region of the spectrum, which in turn could produce less stimulated luminescence. The better response of the White plates could also be because they contained more storage phosphor [20] than the Blue plates and that F ($Br^-$)-centers are more efficiently created in its storage phosphor. Although little or no loss of sensitivity was observed between white and blue X-ray IP's [25,26], we emphasize that in both the earlier X-ray IP and our present neutron IP comparison, the relative measured sensitivities are a combination of all the storage and read-out processes.

We mention finally that the optimal wavelength for photostimulation of Blue NIP's is about 500 nm (Fig. 3), very close to the emission wavelength of Ar lasers (501.4 nm). However even if this wavelength were used the response of the Blue NIP's would still be only 25% that of the White NIP's if the latter were simulated by a He-Ne laser.

To conclude we report here about two important luminescence characteristics of neutron image plate detectors, namely their direct-luminescence spectra as well stimulation spectra of pre-irradiated neutron image plates. Neither one nor the other cannot be measured when the image plate is attached to the image-plate diffractometer. On the other hand, knowledge of these characteristics is absolutely necessary for the correct selection of the filters for detection of fluorescent signal, as well as for the proper selection of the laser source for reading diffraction patterns. Note, that other performance parameters of neutron image plates, such as sensitivity, wide dynamic range, their read-out and fading were reported and discussed in details more than once [15–24].

## 4. Conclusion

The luminescence properties of two types of neutron image plates were evaluated. Their relative efficiencies under X-ray illumination as well as the optimal wavelengths for photostimulation were determined. The PSL response of the Blue NIP is only 25% that of the White NIP, which makes it considerably less attractive for neutron crystallography where the resolution requirements may be relaxed.

## Acknowledgement

We are greatly indebted to Prof. H. von Seggern for the possibility to perform these measurements in his department and for helpful discussions.

## References

[1] K. Takahashi, K. Kohda, J. Miyahara, Y. Kanemitsu, K. Amitani, S. Shionoya, J. Lumin. 31&32 (1984) 266–268.
[2] D.M. De Leeuw, T. Kovats, S.P. Herko, J. Electrochem. Soc. 134 (1987) 491–493.
[3] H. von Seggern, A. Meijerink, T. Voigt, A. Winnacker, J. Appl. Phys. 66 (1989) 4418–4424.
[4] H.H. Rüter, H. von Seggern, R. Reininger, V. Saile, Phys. Rev. Lett. 65 (1990) 2438.
[5] M. Thoms, H. von Seggern, A. Winnacker, Phys. Rev. B 44 (1991) 924.
[6] A. Meijerink, G. Blasse, J. Phys. D: Appl. Phys. 24 (1991) 626.
[7] P.F. Braslavets, A. Kalniņš, I. Pļaviņa, A.I. Popov, B.I. Rapoport, A. Tāle, Phys. Status Solidi (b) 170 (1992) 395–401.
[8] L.E. Trinkler, M.F. Trinkler, A.I. Popov, Phys. Status Solidi (b) 180 (1993) K31–K34.
[9] E.A. Kotomin, A.I. Popov, A. Stashans, J. Phys.: Condens. Matter 6 (1994) L569.
[10] A. Harrison, M.T. Harrison, G.P. Keogh, R.H. Templer, A.S. Wills, Phys. Rev. B 53 (1996) 5039.
[11] S.A. Chernov, L. Trinkler, A.I. Popov, Radiat. Eff. Defects Solids 143 (1998) 345–355.
[12] M.A. Monge, R. Gonzalez, J.M. Santiuste, R. Pareja, Y. Chen, E.A. Kotomin, A.I. Popov, Phys. Rev. B 60 (1999) 3787.
[13] M.A. Monge, R. Gonzalez, J.M. Santiuste, R. Pareja, Y. Chen, E.A. Kotomin, A.I. Popov, Nucl. Instrum. Methods Phys. Res., Sect. B 166 (2000) 220–224.
[14] A. Lushchik, E. Feldbach, A. Frorip, K. Ibragimov, I. Kuusmann, C. Lushchik, J. Phys.: Condens. Matter 6 (1994) 2357.
[15] A.V. Sidorenko, A.J.J. Bos, P. Dorenbos, C.W.E. van Eijk, P.A. Rodnyi, I.V. Berezovskaya, V.P. Dotsenko, A.I. Popov, J. Appl. Phys. 95 (2004) 7898–7902.
[16] C. Wilkinson, A. Gabriel, M.S. Lehmann, T. Zemb, F. Né, Proc. SPIE 1737 (1992) 324.
[17] H. Niimura, Y. Karasawa, I. Tanaka, J. Miyahara, K. Takahashi, H. Saito, M. Hidaka, Nucl. Instrum. Methods A 349 (1994) 521–525.
[18] F. Cipriani, J.-C. Castagna, L. Claustre, C. Wilkinson, M.S. Lehmann, Nucl. Instrum. Methods A 392 (1997) 471.
[19] C. Wilkinson, J.A. Cowan, D.A.A. Myles, F. Cipriani, G.J. McIntyre, Neutron News 13 (2002) 37.
[20] M. Thoms, M.S. Lehmann, C. Wilkinson, Nucl. Instrum. Methods A 384 (1997) 457–462.
[21] G.J. McIntyre, M.H. Lemée-Cailleau, C. Wilkinson, Physica B 385 (2006) 1055–1058.
[22] M.P. Blakeley, Crystallogr. Rev. 15 (2009) 157–218.
[23] C. Wilkinson, P. Schobinger-Papamantellos, D. Myles, L.D. Tung, K.H.J. Buschow, J. Magn. Magn. Mater. 217 (2000) 55.
[24] S. Tazaki, K. Neriishi, K. Takahashi, M. Etoh, Y. Karasawa, S. Kumazawa, N. Niimura, Nucl. Instrum. Methods A 424 (1999) 20.
[25] M. Sato, Y. Katsube, K. Hayashi, J. Appl. Crystallogr. 26 (1993) 733.
[26] M. Yamamoto, T. Kumasaka, T. Uruga, N. Kamiya, H. Iwasaki, T. Ueki, Nucl. Instrum. Methods A 416 (1998) 314.
[27] A. Kalnins, I. Plavina, A.I. Popov, A. Tale, J. Phys.: Condens. Matter 3 (1991) 1265.
[28] A.I. Popov, I. Plavina, Nucl. Instrum. Methods B 101 (1995) 252–254.
[29] K. Chakrabarti, V.K. Mathur, L.A. Thomas, R.J. Abbundi, J. Appl. Phys. 65 (1989) 2021.
[30] R. Barve, R.R. Patil, N.P. Gaikwad, M.S. Kulkarni, D.R. Mishra, A. Soni, S.V. Moharil, Radiat. Meas. 59 (2013) 73–80.
[31] D. Starick, A.M. Gurvich, M.G. Myagkova, J. Rüdiger, G. Herzog, Nucl. Tracks Radiat. Meas. 21 (1993) 39.
[32] Y. Iwabuchi, C. Umemoto, K. Takahashi, S. Shionoya, J. Lumin. 48–49 (1991) 481.
[33] T. Hangleiter, F.-K. Koschnick, J.-M. Spaeth, R.H.D. Nuttal, R.S. Eachus, J. Phys.: Condens. Matter 2 (1990) 6837.
[34] M.Z. Su, Y.L. Wang, W. Zhao, Z.F. Song, J. Less Common Metals 148 (1989) 241.
[35] H. von Seggern, S. Hesse, J. Zimmermann, G.A. Appleby, X. Meng, C. Fasel, R. Riedel, Radiat. Meas. 45 (2010) 478–484.
[36] C. Hall, I. Kamenskikh, A.M. Gurvich, I.H. Munro, V.V. Mikhailin, J.S. Worgan, J. X-ray Sci. Technol. 6 (1996) 48–62.
[37] E. Radzhabov, V. Otroshok, J. Phys. Chem. Solids 56 (1995) 1–7.
[38] A.R. Lakshmanan, N. Murase, T. Yazawa, J. Qiu, T. Mitsuyu, K. Hirao, W. Hoffmann, Radiat. Meas. 33 (2001) 119–127.
[39] R.S. Eachus, W.G. McDugle, R.H.D. Nuttall, M.T. Olm, F.K. Koschnick, T. Hangleiter, J.M. Spaeth, J. Phys.: Condens. Matter 3 (1991) 9327.
[40] F.K. Koschnick, J.M. Spaeth, R.S. Eachus, J. Phys.: Condens. Matter 4 (1992) 3015.
[41] S. Hesse, H. von Seggern, J. Phys. D: Appl. Phys. 37 (2004) 836.